Electronic Supplementary Material (ESI) for Lab on a Chip.

Supplemental Information

Scalable droplet-based radiosynthesis of [^{18}F]fluorobenzyltriphenylphosphonium cation ([^{18}F]FBnTP) via a "numbering up" approach

Yingqing Lu,[abc] Jeffrey Collins,[ab] Kuo-Shyan Lin,[de] and R. Michael van Dam*[abc]

[a]Crump Institute for Molecular Imaging, University of California Los Angeles (UCLA), Los Angeles, CA, USA

[b]Department of Molecular & Medical Pharmacology, UCLA, Los Angeles, CA, USA

[c]Physics and Biology in Medicine Interdepartmental Graduate Program, UCLA, Los Angeles, CA, USA

[d]Department of Molecular Oncology, BC Cancer Research Institute, Vancouver, British Columbia, Canada

[e]Department of Radiology, University of British Columbia, Vancouver, British Columbia, Canada

Contents

1. Microdroplet reaction chips

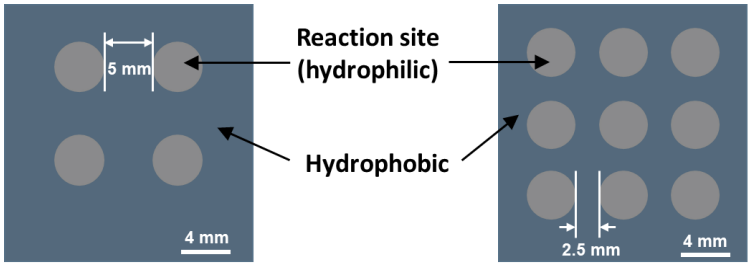

Figure S1. 2×2 and 3×3 multi-reaction chips for high-throughput synthesis optimization and for increasing synthesis scale by pooling the crude products of parallel reactions ("numbering up").

2. Preliminary experiments

Table S1. Preliminary attempts at droplet radiosynthesis of [^{18}F]FBnTP via the Cu-mediated route by adapting literature protocols. **Condition 1** was adapted from the macroscale conditions reported by Zhang *et al.* [1] (i.e. KOTf (1.33 umol), K_2CO_3 (1.81 nmol), $Cu(OTf)_2$ (20 µmol), precursor (4 µmol) in 850 µL of DMF at 110ºC for 20 min). The microscale reaction was performed by scaling down from 850 µL to 10 µL and keep the same reagent ratios, but with increased concentration (~3x). **Conditions 2 and 3** are based on a previously reported droplet-based radiosynthesis of [^{18}F]FDOPA [2] (fluorination reaction) but with [^{18}F]FBnTP precursor instead, and two different amounts of precursor. **Condition 4** is the preliminary droplet condition for [^{18}F]FBnTP synthesis reported in our recent paper [3]. All reactions were performed at 110°C for 5 min.

Condition	1	2	3	4
Reference	1	2	2	3
PTC and base composition (nmol)	KOTf (50) K_2CO_3 (0.0675)	TEAOTf (300) Cs_2CO_3 (10)	TEAOTf (300) Cs_2CO_3 (10)	TEAOTf (300) Cs_2CO_3 (10)
Precursor (µmol)	0.15	0.15	0.45	0.45
Copper reagent (µmol)	$Cu(OTf)_2$ (0.75)	$Cu(Py)_4(OTf)_2$ (0.68)	$Cu(Py)_4(OTf)_2$ (0.68)	$Cu(Py)_4(OTf)_2$ (0.68)
Solvent composition (10 µL reaction)	DMF/Py (96:4, v/v)	DMF/Py (96:4, v/v)	DMF/Py (96:4, v/v)	DMI/Py (96:4, v/v)
Performance (n = 3)				
Starting activity (MBq)	262 ± 4	262 ± 4	262 ± 4	262 ± 4
Collection efficiency (%)	80 ± 4	32 ± 1	33 ± 1	90 ± 1
Residual on pipette tip (%)	1 ± 0	1 ± 1	0.3 ± 0.2	0.4 ± 0.2
Radiochemical conversion (RCC, %)	0	25 ± 1	53 ± 8	92 ± 1
Crude RCY (%)	0	8 ± 0	17 ± 3	83 ± 2

3. Influence of reaction site diameter

Table S2. Comparison of the reaction performance on chips with 4 mm reaction sites (this work) vs 3 mm reaction sites (reported by Jones *et al.* [3]).

	Reaction site diameter (mm)	Number of replicates (n)	RCC (%)	Collection efficiency (%)	Crude RCY (%)
This work[a]	4	3	92 ± 1	90 ± 1	83 ± 2
Previous work[a]	3	4	89 ± 1	97 ± 2	86 ± 2

[a]All reactions were performed as follows. 5 µL of $[^{18}F]F^-$ and 5 µL of TEAOTf (0.3 µmol)/Cs_2CO_3 (0.01 µmol) were dispensed on the reaction site and dried at 105°C for 1 min. The precursor (0.45 µmol) and $Cu(OTf)_2(Py)_4$ (0.68 µmol) in 10 µL of DMI/pyridine (96:4, v/v) were then added and reacted at 110°C for 5 min.

4. Influence of amount of precursor

Table S3. Summary of data acquired when exploring the impact of precursor amount for preparing $[^{18}F]$FBnTP. Each condition was repeated n = 3 times.

Precursor amount (µmol)[a]	RCC (%)	Collection efficiency (%)	Crude RCY (%)
0.15	92 ± 0	89 ± 2	82 ± 2
0.20	96 ± 0	90 ± 4	86 ± 3
0.30	97 ± 0	89 ± 2	86 ± 2
0.45	97 ± 1	90 ± 3	88 ± 3
0.60	99 ± 0	93 ± 2	92 ± 2

[a]All reactions were performed as follows. 5 µL of $[^{18}F]F^-$ and 5 µL of TEAOTf (0.3 µmol)/Cs_2CO_3 (0.01 µmol) were dispensed on the reaction site and dried at 105°C for 1 min. The precursor (amounts indicated) and $Cu(OTf)_2(Py)_4$ (0.68 µmol) in 10 µL of DMI/pyridine (96:4, v/v) were then added and reacted at 110°C for 5 min.

5. Influence of starting activity and volume of $[^{18}F]$fluoride

Table S4. Summary of data acquired when exploring the impact of $[^{18}F]$fluoride volume or starting activity when preparing $[^{18}F]$FBnTP. Precursor amount for these studies was 0.45 µmol. All experiments were performed at relatively low activity (11.7-69.6 MBq).

$[^{18}F]$fluoride volume (µL)	Number of replicates (n)	Starting activity (MBq)	RCC (%)	Collection efficiency (%)	Crude RCY (%)
5	2	11.9 ± 0.3	92 ± 0	92 ± 2	84 ± 2
10	2	23.6 ± 0.4	95 ± 1	92 ± 1	87 ± 1
15	2	34.6 ± 0.3	93 ± 1	92 ± 1	85 ± 0
20	2	45.7 ± 0.8	91 ± 2	90 ± 1	81 ± 2
25	1	56.2	93	90	84
40	2	68.0 ± 2.3	32 ± 27	81 ± 13	24 ± 18

Table S5. Summary of data acquired when exploring the impact of precursor amount in conjunction with higher volume of [^{18}F]fluoride (40 μL) when preparing [^{18}F]FBnTP. All experiments were performed at relatively low activity (58.2-69.6 MBq). Each condition was repeated n = 2 times.

Precursor amount (μmol)	Starting activity (MBq)	RCC (%)	Collection efficiency (%)	Crude RCY (%)
0.45	68.0 ± 2.3	32 ± 27	81 ± 13	24 ± 18
0.60	60.5 ± 1.8	52 ± 1	85 ± 1	44 ± 2
0.75	59.2 ± 1.4	47 ± 3	88 ± 7	41 ± 6
0.90	60.3 ± 1.9	55 ± 12	84 ± 4	47 ± 13
1.05	59.8 ± 0.1	65 ± 5	89 ± 1	57 ± 4

Table S6. Summary of data acquired when exploring the impact of [^{18}F]fluoride volume or starting activity when preparing [^{18}F]FBnTP. Precursor amount for these studies was 0.60 μmol. Experiments were performed over a wider activity range (25.3-1510 MBq).

[^{18}F]fluoride volume (μL)	Number of replicates (n)	Starting activity (MBq)	RCC (%)	Collection efficiency (%)	Crude RCY (%)
5	6	86 ± 47	94 ± 2	91 ± 3	86 ± 4
25	2	710 ± 270	74 ± 7	86 ± 5	63 ± 2
30	2	930 ± 180	73 ± 1	85 ± 1	62 ± 2
40	2	60.5 ± 1.8	52 ± 1	85 ± 1	44 ± 2
42	2	970 ± 770	26 ± 16	89 ± 1	23 ± 14

6. Representative HPLC chromatograms

5.1 The synthesis by pooling two droplet reactions

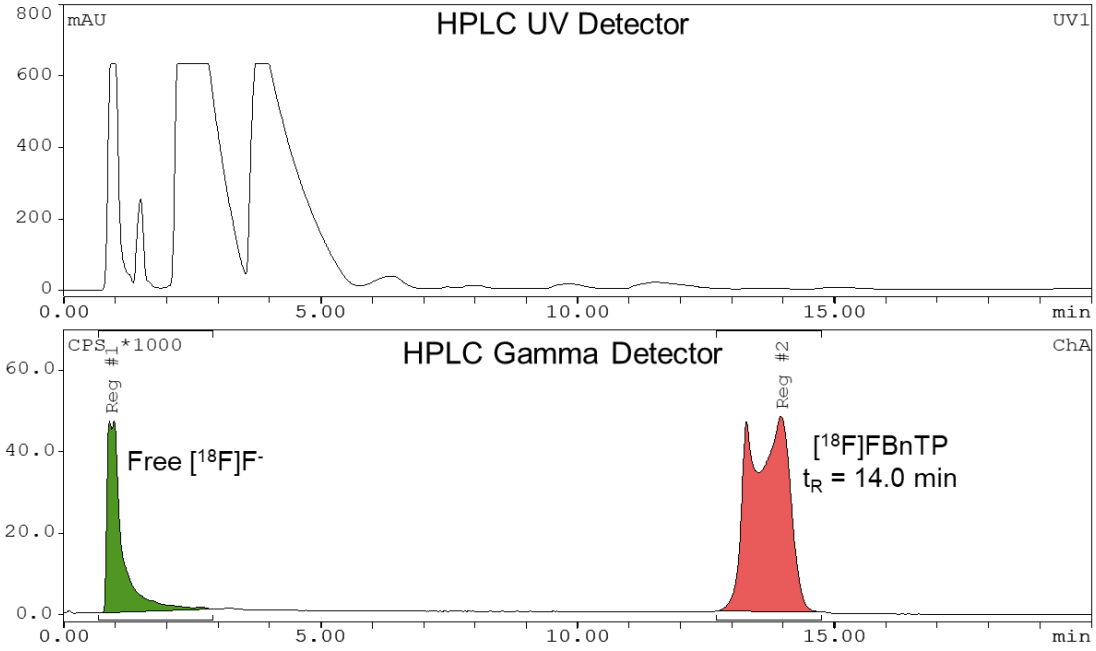

Figure S2. Radio-HPLC chromatogram, during purification on an analytical column, of crude [^{18}F]FBnTP by pooling two droplet reactions. The apparent split in the product peak is an artifact due to saturation of the radiation detector.

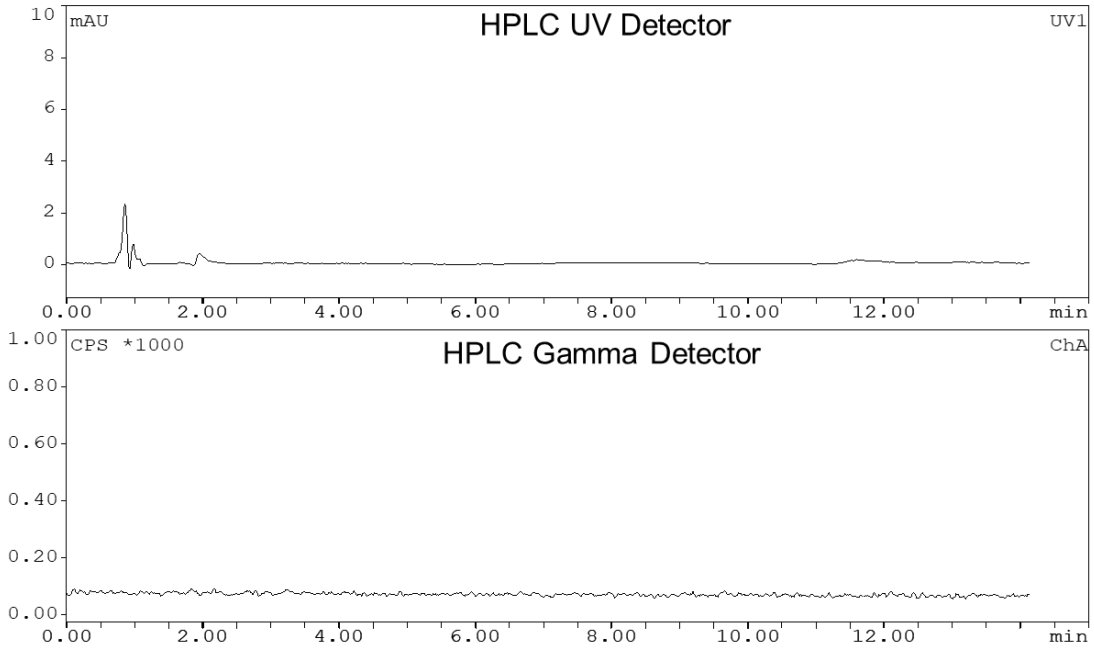

Figure S3. Blank injection of formulation buffer, i.e., saline and EtOH (9:1, v/v).

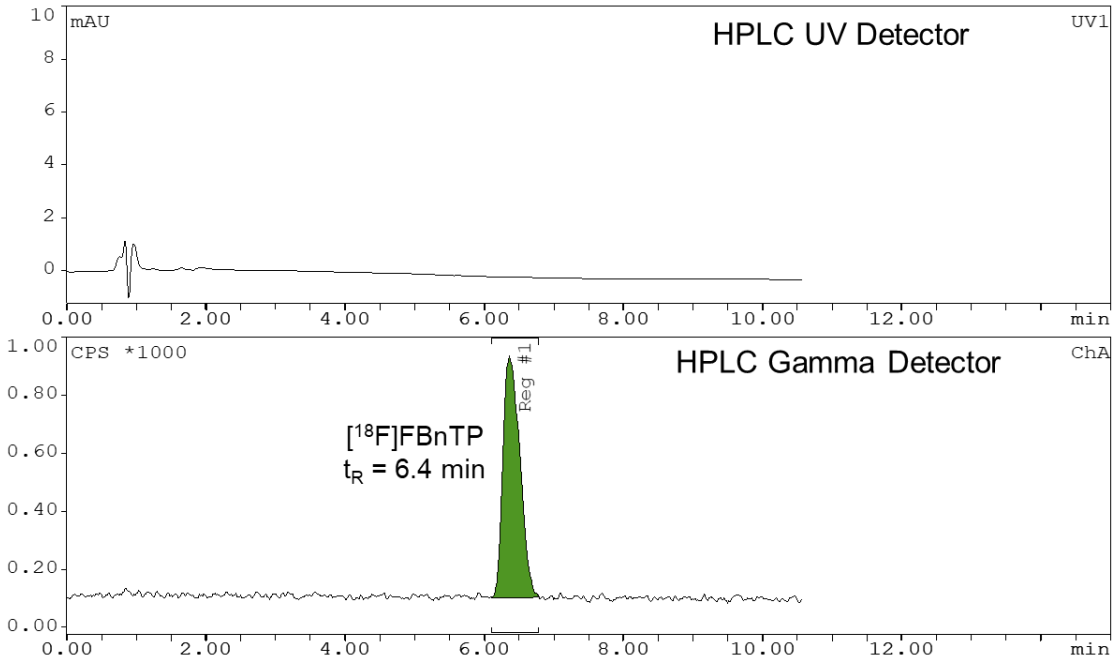

Figure S4. Radio-HPLC chromatogram of formulated [^{18}F]FBnTP (from pooling two droplet reactions).

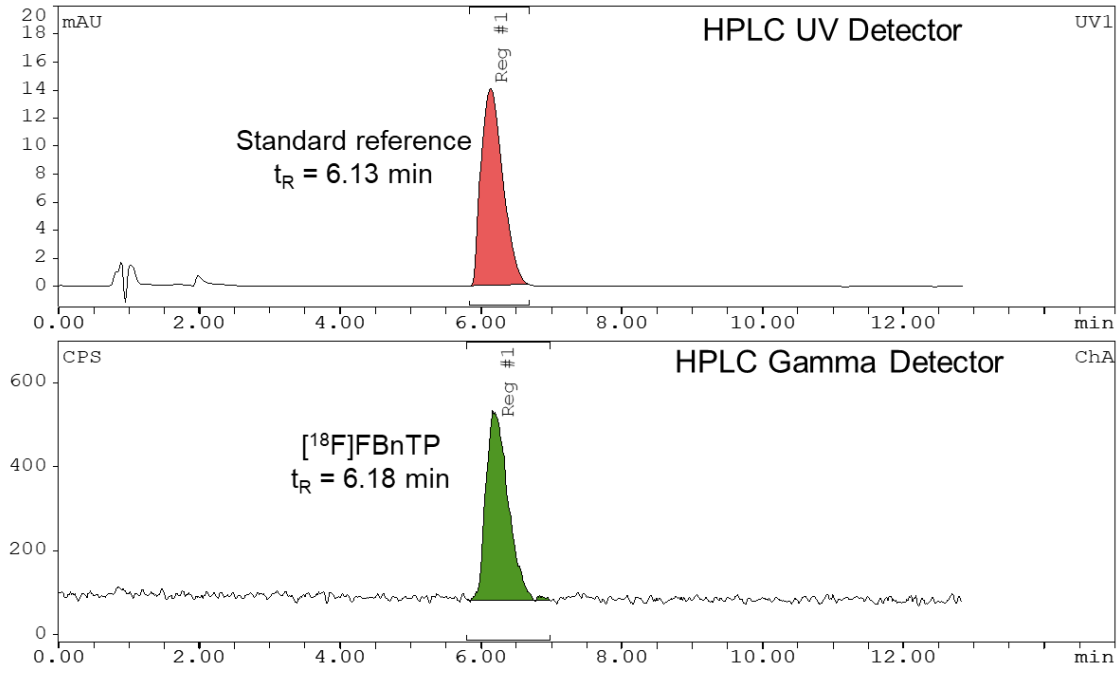

Figure S5. Radio-HPLC chromatogram of co-injection of formulated [^{18}F]FBnTP (from pooling two droplet reactions) and FBnTP reference standard.

5.2 The synthesis by pooling four droplet reactions

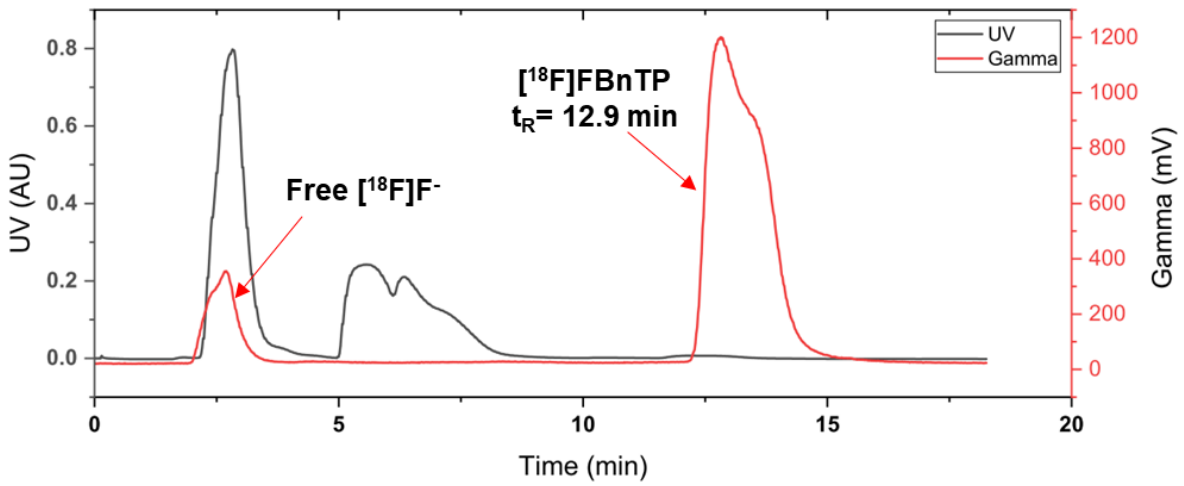

Figure S6. Radio-HPLC chromatogram, during purification on a semi-prep column, of crude [^{18}F]FBnTP by pooling four droplet reactions.

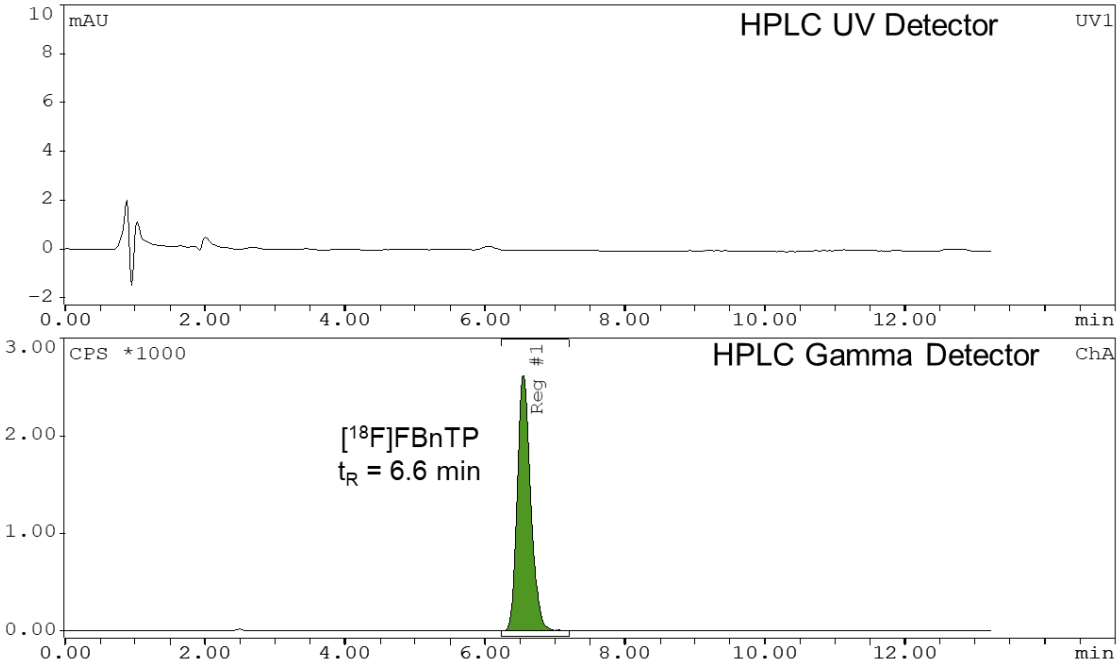

Figure S7. Radio-HPLC chromatogram of formulated [^{18}F]FBnTP (from pooling four droplet reactions).

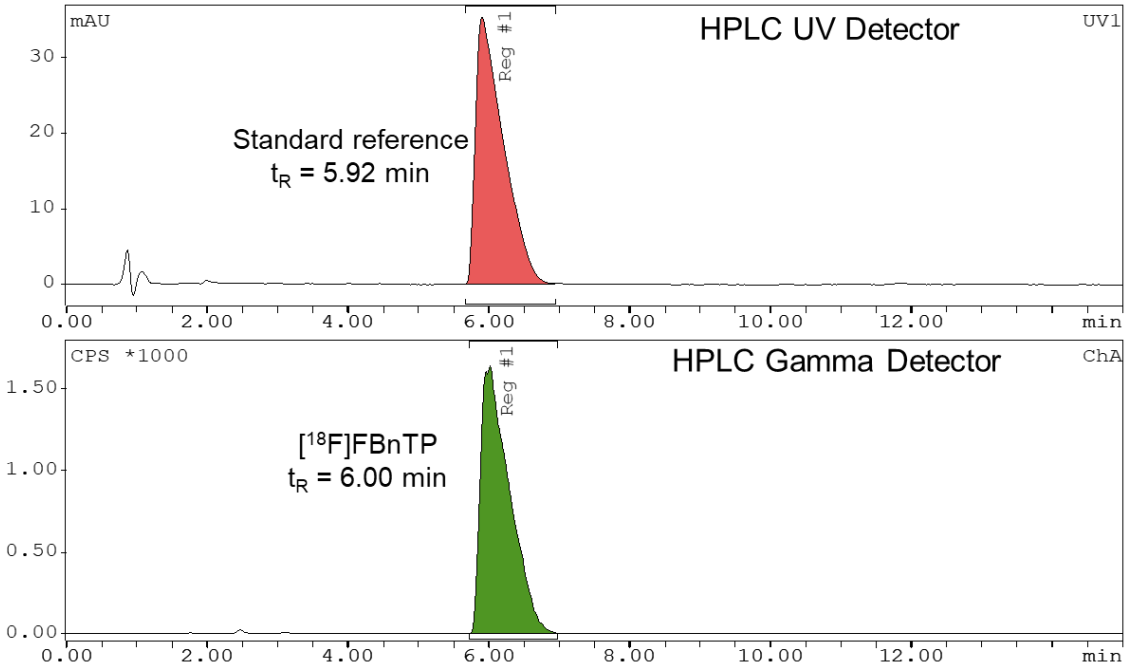

Figure S8. Radio-HPLC chromatogram of coninjection of formulated [^{18}F]FBnTP (from pooling four droplet reactions) and FBnTP reference standard.

7. Molar activity determination

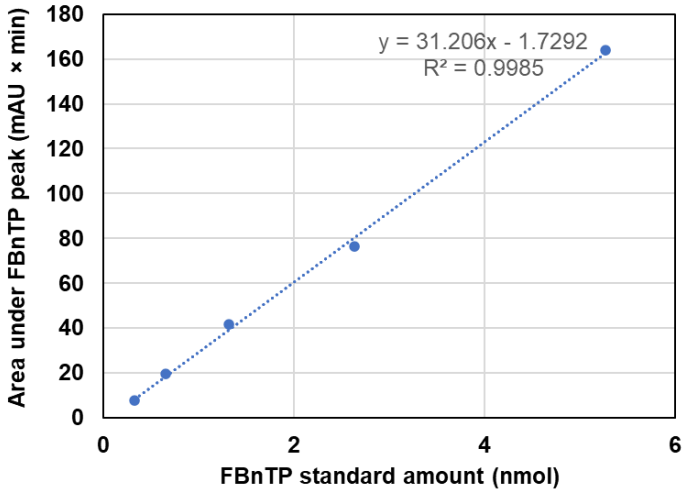

Figure S10. Calibration curve of FBnTP reference standard. UV absorbance was measured at 254 nm.

8. Saturation of gamma detector on HPLC

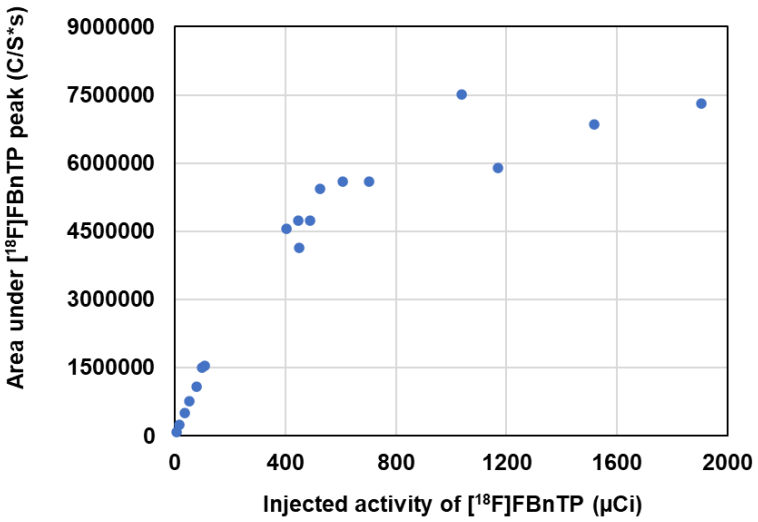

Figure S11. Injected activity of [^{18}F]FBnTP and corresponding obtained signal counts from gamma detector on HPLC.

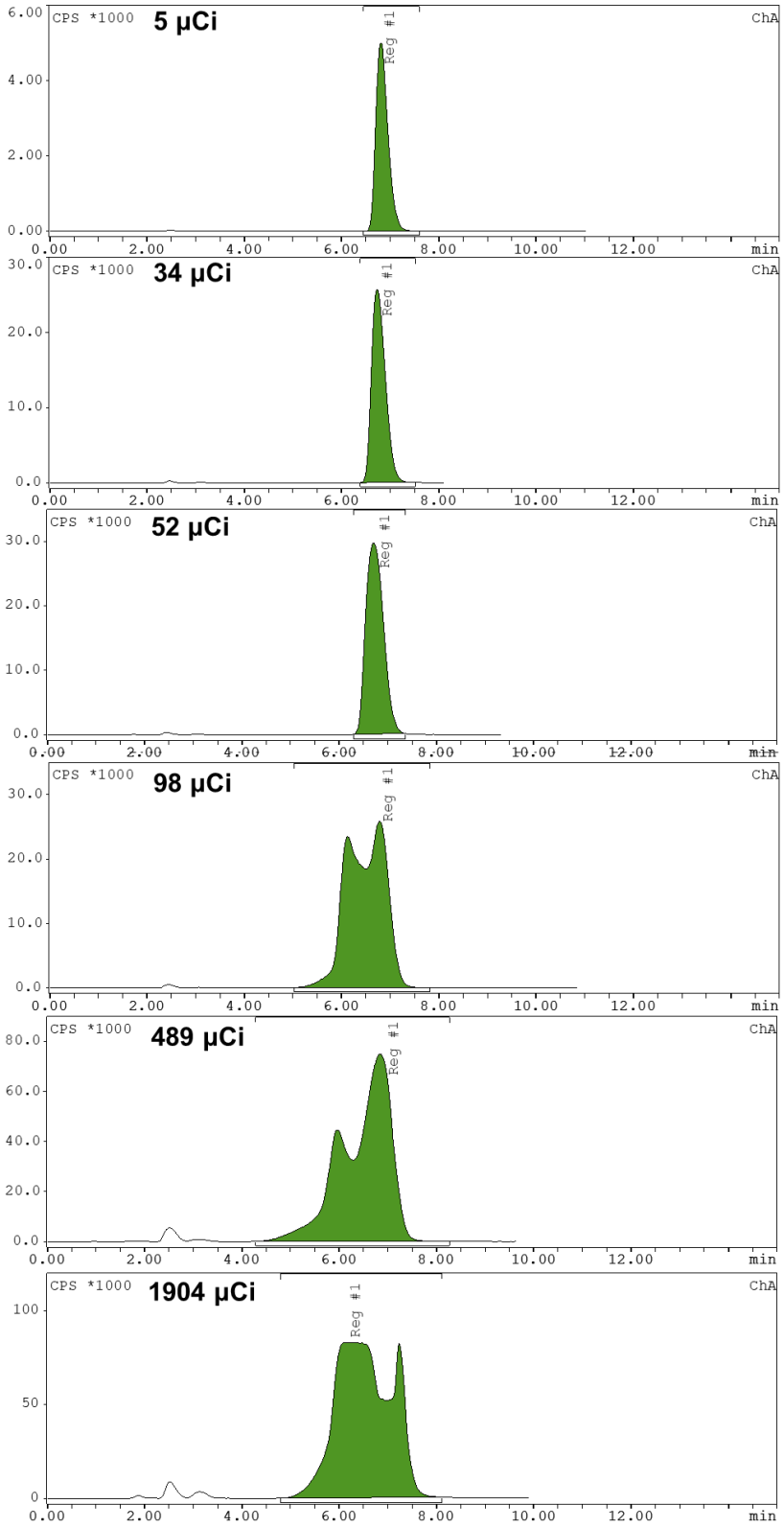

Figure S12. Examples of radio-HPLC chromatograms (gamma detector) for samples of [^{18}F]FBnTP diluted by different amounts. The total activity in the ~180 µL injection is shown for each chromatogram, with decay-correction to the actual time at which sample reached detector.

9. References

1 X. Zhang, F. Basuli and R. E. Swenson, *J Label Compd Radiopharm*, 2019, **62**, 139–145.
2 Y. Lu and R. M. van Dam, *Nucl. Med. Biol.*, 2021, **96–97**, S15–S16.
3 J. Jones, V. Do, Y. Lu and R. M. van Dam, *J. Chem. Eng.*, 2023, **468**, 143524.